Direct Observation of the Spontaneous Emission of the Hyperfine Transition $F = 4$ to $F = 3$ in Ground State Hydrogenlike $^{165}Ho^{66+}$ in an Electron Beam Ion Trap

José R. Crespo López-Urrutia, P. Beiersdorfer, Daniel W. Savin, and Klaus Widmann
Lawrence Livermore National Laboratory, Livermore, California 94550
(Received 16 February 1996)

We report the first direct laboratory measurement of the spontaneous emission due to the hyperfine splitting of the ground state of a highly charged hydrogenlike ion excited by electron collisions. The transition between the $F = 4$ and $F = 3$ levels of the $1s\,^2S_{1/2}$ configuration of hydrogenlike $^{165}Ho^{65+}$ was observed and its wavelength was determined to 5726.4 ± 1.5 Å. After taking into account relativistic, nuclear charge distribution, Bohr-Weisskopf, and QED corrections, we observe a significant deviation from commonly tabulated values of the nuclear dipole magnetic moment of this nucleus. [S0031-9007(96)00712-0]

PACS numbers: 32.10.Fn, 12.20.Fv, 21.10.Ky, 32.30.Jc

Measurements of the hyperfine splitting of the ground state of hydrogen provide a very sensitive tool to explore QED and nuclear contributions to the electron energy. Hydrogenlike ions allow an extension into a region in which these contributions scale to larger values. The 1*s* electron of a highly charged ion probes the structure of the nucleus more deeply, due to its Coulomb field, enabling a very sensitive test of theory in strong fields. This method complements measurements of muonic atoms, where the muon probes the magnetic field distribution of the nucleus (Bohr-Weisskopf effect). While the spontaneous 1*s* hyperfine transition in H, D, and He^+ has been observed in radio astronomy, laboratory measurements in hydrogen and low-*Z* hydrogenlike ions have to rely on stimulated emission using a maser setup due to the extremely long lifetime of the upper hyperfine level (1.1×10^7 yr for H) [1,2]. This technique was successful in measuring the splitting in H, D, T, and He^+. Laser pumping has recently been applied to H-like Bi^{82+} circulating at nearly 60% the speed of light in a heavy-ion storage ring [3] resulting in the first measurement of the hyperfine splitting in multiply charged ions. Here laser fluorescence was detected as the laser frequency was tuned in and out of resonance with the Doppler-shifted transition. Accurate *a priori* knowledge of the hyperfine transition is required, lest a prohibitively large scan in the laser frequency be performed.

We measure the $F = 4$ to $F = 3$ hyperfine transition of the 1*s* ground level of H-like $^{165}Ho^{66+}$ using passive emission spectroscopy. The measured wavelength of 5726.4 Å differs 89 Å from a recent calculation [4]. The fact that the transition is excited by electron collisions and the relative ease of the present technique, in principle, opens the upper half of the periodic table to scientific scrutiny.

Hydrogenlike holmium ions are produced and stored in a high energy electron beam ion trap (SuperEBIT) [15] by an electron beam of variable energy axially compressed by a high magnetic field. The SuperEBIT has been used to perform very accurate spectroscopic measurements of highly charged ions in the x-ray regime [6], while no such measurements have been made in the optical. The possibility of performing spectroscopy of highly charged ions in the visible on a low-energy EBIT was demonstrated only recently by Morgan *et al.* [7], who measured optical transitions in V-like and Ti-like Xe and Ba ions in the NIST EBIT.

A schematic of the SuperEBIT optical spectrometer is shown in Fig. 1. It consists of a prism spectrograph (Steinheil) with an aperture of $f/9$, and a cryogenically cooled charge coupled device (CCD) camera detector. This setup differs greatly from the scanning monochromator with photomultiplier tube (PMT) setup described in [7]: (a) It allows simultaneous coverage of the whole visible spectrum, providing much faster data acquisition. (b) It also has lower noise: typical PMTs have several tens of counts per second of dark current, versus few counts per hour for the CCD detector used here, recording a single line on a region of roughly 400 pixels surface. (c) The trap is spatially resolved in the vertical and horizontal directions, giving information about the spatial distribution of the ions.

A port on the side of the vacuum chamber with a quartz window allows direct view of the beam in the trap region through a slotted aperture in the drift tube. The electron beam and the apparatus symmetry axis are aligned vertically. The beam is stigmatically imaged by two achromats ($f1 = 655$ mm, $f2 = 250$ mm, demagnification 2.6 times) on the focal plane of the spectrograph, where the CCD detector is placed (1024 × 1024 pixels of

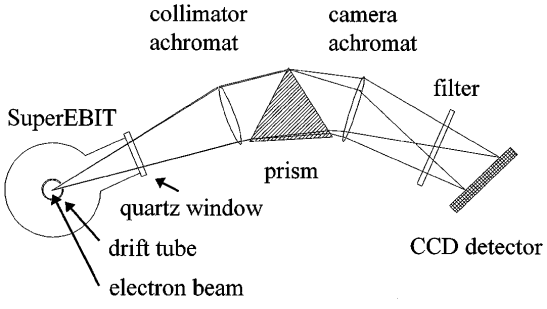

FIG. 1. Stigmatic spectrograph arrangement.

 0031-9007/96/77(5)/826(4)$10.00

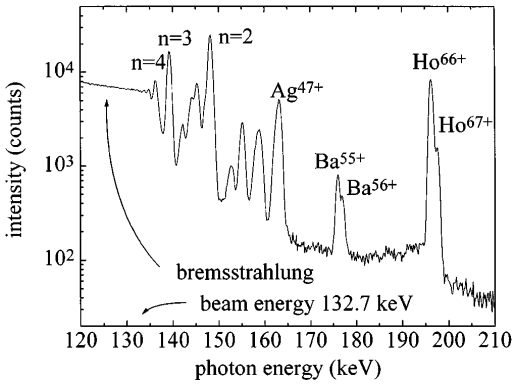

FIG. 2. X-ray spectrum from SuperEBIT with the hydrogenic and bare Ho radiative recombination lines. Only emission above 120 keV photon energy is shown.

24 μm side length). A prism spectrograph was chosen because of its high efficiency, low level of scattered light, and the needs of our geometrical arrangement. The spectral range covered in a single image was from 4175 to 6900 Å. The narrow beam itself (70 μm diameter) forms the entrance slit in this arrangement. The stigmatic imaging spatially resolves the vertical structure of the trap (0.1 mm resolution) allowing to distinguish between line radiation emitted by cooling gas atoms and trapped ions. Radiation from the coupling gas appears as short lines in a region of 7 mm length in the center of the trap, where an atomic beam from the gas injector crosses the electron beam at 90°. Here electron collisional excitation and fast radiative decay of the neutral atoms take place, and a large number of lines can be observed. Some atoms are also ionized and trapped. Trapped ions fill the whole trap length, and are excited and deexcited anywhere in this volume. The visible transitions from trapped ions thus appear as lines that are 20 mm long. The spatial resolution is therefore important to determine the nature of the light emitting species.

The ion temperature, estimated to be less than 2 keV [8], does not limit the spectral resolution. The observed linewidth of 2.5 pixels FWHM is purely instrumental. The quantum efficiency at the wavelength of interest is higher than 65%. A cutoff filter (BG38) is used to reduce the near-IR stray light background above 6700 Å. Its transmission at 5730 Å, including the reflection and absorption losses of the other optical elements and windows. The total detection efficiency of the system, after taking in consideration a solid angle collection efficiency of 7×10^{-4} is around 2.5×10^{-4}. To minimize background, all possible light sources in the chamber (ion pressure gauges) had to be turned off. The largest source of background is the thermal radiation from the indirectly heated electron gun cathode, which is reduced by the cutoff filter. Background and the atomic line emission from the gas injector are eliminated by subtracting from every spectrum taken with holmium ions present in the trap another one taken without holmium ions, under otherwise identical conditions. This measurement cycle is repeated every 2 h. The standard deviation of the dark current counts per pixel after 1 h exposure is less than two and is negligible compared with the statistical fluctuations of the background.

The trap is simultaneously monitored by two germanium detectors. They register the emitted x rays which include the K_α line from the trapped ions, the electron bremsstrahlung continuum and the radiative recombination (RR) lines produced by beam electrons captured into different open shells of the ions (cf. Fig. 2). We used these spectra to determine the ionic species and the charge balance in the trap. With the holmium MEVVA on, at a beam energy of 132 keV and 285 mA beam current, the He-like Ho^{65+} ion was the most abundant species in the trap (40%) followed by Li-like Ho^{64+} (25%). The concentration of H-like Ho^{66+} was 6%, that of bare Ho^{67+} around 0.5%. Lower charge states made up the rest. With the MEVVA off, the trap is filled by slow accumulation over several minutes of Ag, Ba, Au, W, and other heavy elements emanating mainly from the heated cathode and by ion sputtering from the walls. During the holmium runs, interference from this process is avoided by dumping the trap every 20 s and refilling it with a new MEVVA discharge. For the background runs without Ho, no dumping is performed in order to load the trap with high-Z impurities. The gas injector runs always under the same conditions, so that those neutral lines from the gases seen in the individual spectra disappear completely after subtraction of consecutive runs with and without holmium. Ideally, after background subtraction, one would obtain a flat image where all values are close to zero within ten counts. However, during the long integration times (1 h) used for the individual exposures, a number of cosmic rays are also detected by the CCD. Each of these events produces hundreds or thousands of counts in a single pixel or in a straight path along several pixels. Their contribution is largely reduced by using a computer program which resets to zero all pixels showing deviations from 0 larger than 10 counts, since the photon signal expected is much weaker, only one or two counts per pixel/h. Around 0.3% to 1% of the pixels are reset in this way. This method does not create any artifacts, since the distribution of the cosmic events is stochastic. After performing this procedure, the remaining baseline fluctuation is mainly due to the statistical variation of the thermal radiation background in the trap.

To obtain spectra from the two-dimensional images, the pixel counts on the CCD detector are integrated along one dimension. This can be done with minimal loss of spectral resolution since the image of the vertically oriented spectral lines has a deviation from the straight line of less than two pixels over 200 pixels length. The result of the addition of 18 background corrected spectra (36 h of data) is displayed in Fig. 3. A single feature at 5726.4 ± 1.5 Å with a peak height 10 times larger than the standard deviation of the background line and a FWHM of 15 Å appeared. The total number of counts above the background over the line profile was around 4000. We attribute this feature to the hyperfine transition in Ho^{66+}.

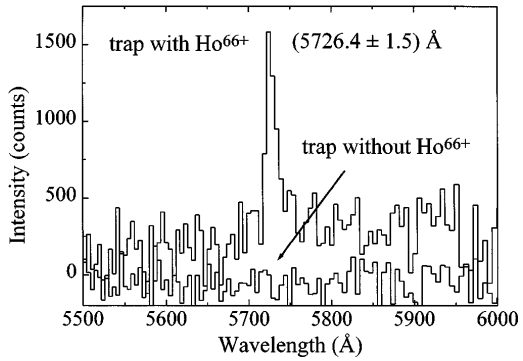

FIG. 3. The $F = 4$ to $F = 3$ hyperfine transition in hydrogenlike Ho^{66+} and its baseline.

To exclude the possibility that the line was emitted by a lower charge state, the experiment was repeated, making sure that no H-like Ho^{66+} could be produced, while keeping the other charge states in the trap more or less unchanged. The beam energy was lowered below the ionization potential of He-like Ho^{65+} (63 keV). The x-ray spectra showed that the He-like ion density was still highest, while there was no H-like Ho present and that lower charge states were present in a slightly larger concentration than before. Again, spectra with an without holmium were subtracted from each other. The resulting spectra displayed no indication of any line at any position throughout the range of observation (4175–6700 Å). Since the only difference in the species present in these spectra compared to the first series was the absence of H-like Ho^{66+}, it was concluded that the observed line was emitted by H-like Ho^{66+} ions.

The possibility that the observed line was populated by charge exchange processes between neon atoms from the gas injector and bare holmium can be excluded for two reasons. First, the ionization energy of the neon used for the cooling in the gas injector would have populated n levels ($n = 25$) lower than those Rydberg levels in Ho^{66+} with suitable energy differences ($n = 41-33$) to produce visible light. Second, this process would have lead also to an yrast chain of several cascading visible lines with decreasing wavelength. So a line at (roughly) 5700 Å would have lines at 5300, 4800, 4500, and 4200 Å accompanying it; that is, more than one line would have been observed. Population of such high Rydberg levels by radiative recombination of beam electrons from the bare Ho^{67+} to generate Ho^{66+} can be excluded for the same reason. In fact, radiative recombination populates mainly the low-lying states of the final ion, and is so likely to populate the upper hyperfine level.

Observation of the $F = 4$ to $F = 3$ hyperfine transition is expected because of several reasons. The trap contains a suitable number of bare and H-like Ho ions. The recombination lines of those two species in the Ge detector were recorded at a rate of more than 10 000 counts/h. The bare Ho^{67+} alone accounted fro roughly 2000 counts/h. Two main processes are expected to populate the upper F level of the H-like ion. The most important is collisional ionization of He-like ions, where one of the two 1s electrons is removed leaving a H-like ion behind with similar probability for population in either the $F = 4$ or $F = 3$ state. In ionization equilibrium (reached within 2 s as determined by time-resolved x-ray spectra), the ionization rate is balanced by the radiative recombination rate of H-like to He-like (ignoring other recombination processes). We can therefore estimate the ionization rate populating the $F = 4$ level from the observed radiative recombination photons and find that is should produce 190 counts/h in the optical spectrograph with the ratio of the solid angles of the Ge detector and the spectrograph. The second process is radiative recombination of beam electrons with bare Ho, also populating $F = 4$ and $F = 3$ nearly evenly. The rate estimated here from the x-ray signal is 35 counts/h. By contrast, collisional excitation requiring a spin flip is far less probable than these two mechanisms and can be neglected. With these processes, a spontaneous emission count rate for the hyperfine transition about 225 counts/h can be expected. This result is consistent with the observed count rate of 220 counts/h.

We estimate the radiative lifetime of the $F = 4$ level from the measured value for the Bi^{82+} hyperfine transition of 0.34 ms [3] and assuming a Z^9 scaling law [2] to be roughly 2–3 ms. This gives a transition rate of 500/s, which is much faster than the collisional deexcitation rate (roughly 10/s) at the present electron beam density. Therefore, collisional deexcitation of the upper level does not affect the result significantly.

The wavelength calibration requires a line source at the position of the beam. We use neutral atoms from the gas injector excited by the electron beam at low energies to generate a large number of calibration lines. Possible instrument shifts were monitored by observing the position of the NeI line at 5852.48 Å, which was still weakly visible at beam energies of 132 keV. The wavelength measurement accuracy of 250 ppm is currently limited by counting statistics and calibration uncertainties. Our experimental result of 5726.4 ± 1.5 Å (air) corresponds to a 5727.9 ± 1.5 Å vacuum wavelength and an energy difference between the $F = 4$ and $F = 3$ levels of 2.1645 ± 0.0006 eV.

The energy difference Δ between two neighboring F levels in a H-like ion is (Shabaev [4])

$$\Delta = \frac{\alpha^4 Z^3}{n^3}\,\frac{\mu_I}{I}\,\frac{m_e}{m_p}\,\frac{(I+j)}{j(j+1)}\,\frac{m_e c^2}{(2l+1)} \times [A(1-\delta)(1-\varepsilon)+\kappa_{\rm rad}], \quad (1)$$

with the following terms: α, fine-structure constant; Z, nuclear charge; n, j, l; principal, total moment, and orbital moment electron quantum numbers; μ_I, nuclear magnetic moment; m_e, m_p, electron, proton mass; I, nuclear spin; A, relativistic factor; δ, nuclear charge distribution

correction; ε, nuclear magnetization distribution (Bohr-Weisskopft) correction; $\kappa_{\rm rad}$, QED radiative correction. Using this formula, but neglecting QED corrections, he predicts a vacuum wavelength of 5639 Å (air wavelength 5637.4 Å), with an uncertainty of at least 40 Å due to the uncertainties in the μ_I value quoted. This value differs significantly from our measured value, i.e., by 89 Å. Two dominant QED corrections have recently been calculated [9,10]. Based on the calculations of the self-energy correction by Persson *et al.* [9], we estimate for $Z = 67$ a -19.3 meV shift. The vacuum polarization was given by Schneider *et al.* in [10]. From their work we estimate this contribution to be 9.4 meV. The total net QED correction therefore is -9.9 meV, or 27 Å. Even after including the shift from QED, there is still a difference of 62 Å between our measurement and the calculated wavelength. Shabaev's [4] calculation uses a value for the nuclear magnetic moment of ^{165}Ho of $4.173(27)\mu_N$ tabulated by Lederer and Shirley in [11] and based on a measurement by the atomic beam resonance method [12] of $4.094(44)\mu_N$ (without diamagnetic correction), later recalculated in [13] to $4.128(27)\mu_N$ (without diamagnetic correction). This value is cited in the literature as $4.160(27)\mu_N$ or $4.173(27)\mu_N$ depending on the size of the diamagnetic correction employed. The evaluation of the original data seemed nonetheless uncertain. A newer measurement was performed by Nachtsheim [14] resulting in $4.132(5)\mu_N$ (corrected), with a 5 times smaller uncertainty. This value is compiled in the review of Peker [15]. Using this value in Eq. (1) and adding the above mentioned QED corrections, we obtain a transition energy of 2.1675 eV, and a vacuum wavelength of 5720.15 Å. This differs from our measured vacuum wavelength (5727.9 $\pm$ 1.5) Å by only 0.13%. We emphasize that this good agreement was reached only using the updated value for the nuclear magnetic moment and the QED corrections. In the case of Bi^{82+}, Shabaev predicts [4] (no QED) a wavelength of 2412 Å, while the measurement at GSI was 2438.7 Å, a discrepancy of 1.1%. A more refined calculation for Bi^{82+} [16] leads to a value of 2419.8 Å, with a smaller discrepancy of 0.8%, and a third one [17], taking nuclear many-body corrections into account, gives an even closer prediction of 2435.4 Å (0.13% discrepancy).

The question of the accurate determination of the nuclear magnetic moment of holmium remains open. A precision measurement of the hyperfine splitting can at present be used only for testing the sum of the contributions from the nuclear magnetic moment, nuclear size effects, and QED. Hyperfine measurements along the isoelectronic sequence and for different isotopes can be used to determine the size of the QED contributions, which follow well-known scaling laws, with high accuracy. Determinations of the nuclear magnetic moment from the 1*s* hyperfine transition measurements, thus, seems within reach. Such measurements would avoid uncertainties in the evaluation of the atomic diamagnetism that may affect many of the values of the tabulated nuclear magnetic momenta.

We have observed the hyperfine transition of the ground state of the hydrogen-like Ho^{66+}. This is one of the few measurements of such transitions, the second involving a highly charged ion and the first from ions excited by electron collisions. The experimental accuracy of the measured wavelength conflicts with a widely cited value of the nuclear magnetic dipole moment of ^{165}Ho of $4.173(27)\mu_N$ and agrees well with another independent measurement of $4.132(5)\mu_N$. The measurement confirms the magnitude of the different corrections used in the prediction of this hyperfine transition. The experimental method can be readily applied to other highly charged ions with hyperfine splitting in the visible or UV range; an extension to the IR or microwave seems also feasible. Future possibilities include the use of laser spectroscopy to determine the lifetime since the count rate at the present is too low to allow its measurement with meaningful accuracy.

Discussions with Thomas Kühl are greatly acknowledged. This work was in part supported by the Office of Basic Energy Sciences and was performed under the auspices of the U.S. DOE by Lawrence Livermore National Laboratory under Contract No. W-7405-ENG-48.

[1] L. Essen, R. W. Donaldson, M. J. Bangham, and E. G. Hope, Nature (London) **229**, 110 (1971).
[2] R. J. Gould, Astrophys. J. **423**, 522 (1994).
[3] I. Klaft *et al.*, Phys. Rev. Lett. **73**, 2425 (1994).
[4] V. M. Shabaev, J. Phys. B **27**, 5825 (1994).
[5] D. A. Knapp *et al.*, Nucl. Instrum. Methods Phys. Res. Sect. A **334**, 305 (1993).
[6] P. Beiersdorfer, D. Knapp, R. Marrs, S. R. Elliot, and M. Chen, Phys. Rev. Lett. **71**, 3939 (1993).
[7] C. A. Morgan *et al.*, Phys. Rev. Lett. **74**, 1716 (1995).
[8] P. Beiersdorfer, V. Decaux, S. R. Elliot, K. Widmann, and K. Wong, Rev. Sci. Instrum **66**, 303 (1995).
[9] H. Persson *et al.*, Phys. Rev. Lett. **76**, 1433 (1996).
[10] S. M. Schneider, W. Greiner, and G. Soff, Phys. Rev. A **50**, 118 (1994).
[11] E. Browne *et al.*, in *Table of Isotopes*, edited by C. M. Lederer and V. S. Shirley (Wiley, New York, 1978), 7th ed.
[12] R. A. Haberstroh, T. I. Moran, and S. Penselin, Z. Phys. **252**, 421 (1972).
[13] W. Dankwort and J. Ferch, Z. Phys. **267**, 239 (1974).
[14] G. Nachtsheim, Ph.D. thesis, Universitãt Bonn, Bonn, 1980 (unpublished).
[15] L. K. Peker, Nucl. Data Sheets **50**, 137 (1987).
[16] L. N. Labzowski, W. R. Johnson, G. Soff, and S. M. Schneider, Phys. Rev. A **51**, 4597 (1995).
[17] M. Tomaselli, S. M. Schneider, E. Kankeleit, and T. Kühl, Phys. Rev. C **51**, 2989 (1995).